

TEMPERATURE INFLUENCE ON THE LACTOSE CAPPED METAL SULPHIDE NANOPARTICLES

T. P. MOFOKENG^a, G. MABENA^a, M. J. MOLOTO^a, P. M. SHUMBULA^b,
K. P. MUBIAYI^a, P. NYAMUKAMBA^{a*}

^a*Department of Chemistry, Vaal University of Technology, Private Bag X021
Vanderbijlpark, 1900, South Africa*

^b*Advanced Materials Division, Mintek, Private Bag X3015, Randburg, 2125,
South Africa*

Metal sulphide nanoparticles are materials with good optical properties and make them useful in biological, biomedical fields for antibacterial, antifungal and drug related work. The paper reports a simple green synthesis of zinc sulphide (ZnS), copper sulphide (CuS) and iron sulphide (FeS) nanoparticles using lactose as the capping agent via a one-step colloidal method. The synthesized nanoparticles were characterized by X-Ray Diffraction (XRD), Transmission Electron Microscope (TEM), UV-Vis spectroscopy, Photoluminescence spectroscopy (PL) and Fourier Transform Infrared spectroscopy (FTIR). The XRD analysis confirmed a cubic crystalline phase for ZnS nanoparticles, hexagonal phase for CuS nanoparticles while FeS nanoparticles were amorphous. The UV-Vis spectra showed that all the absorption peaks were blue shifted from their bulk band edges. The room temperature PL showed that the synthesized nanoparticles were red shifted from their respective UV-Vis spectra. The morphology of the particles was not affected by temperature; however the size of the particles increased with increase in temperature. FTIR spectra confirmed the binding of lactose to the surface of the nanoparticles and solubility tests conducted on these nanoparticles showed that particles synthesised at the highest temperature were soluble for CuS and FeS nanoparticles.

(Received June 26, 2017; Accepted August 25, 2017)

Keywords: Iron sulphide, Copper sulphide, Zinc sulphide, Nanoparticles, Lactose capped, Temperature

1. Introduction

The incorporation of semiconductor nanoparticles or QDs into biological systems often requires strategies for the manipulation of the ligands bound to the surface of the QDs in order to make them water-soluble and biocompatible. This is very important for compatibility with living tissues or in a living system by being neither toxic nor injurious or physiologically reactive [1]. Quantum dots must be rendered water-soluble through the modification of their surface in preparation for biological applications [2]. However, high-quality QDs are mainly prepared using heavy metals like copper, zinc, and iron, of which their long-term toxicity is currently unknown. Thus, much of the recent research efforts have been on developing new strategies to fabricate nanomaterials with carbohydrates [3]. Barrientos et al. [4] used oligosaccharide carbohydrates as capping ligands because of their potential applications in the design and development of nanoscale devices and nanosensors for biomedical applications. Carbohydrates contain many hydroxyl and carbonyl groups; these groups offer sugar coated nanoparticle with unique H-bonding capabilities in constructing supramolecular architecture. Upon surface coating with nanoparticles they provide attractive nano-construction abilities for building smart nanomaterials [5].

Despite the large number of applications, there are only very few reports on direct synthesis of metal sulphide nanoparticles in a lactose or starch matrix. In this study, metal sulphide

*Corresponding author: daddypardy@gmail.com

nanoparticles were synthesized using lactose as a capping agent. Lactose is a carbohydrate molecule that has a potential to enable specific targeting to the surface of the nanocrystals and grant water solubility and biocompatibility, which is necessary for their safe use in bio-based applications.

2. Methodology

2.1. Materials

Zinc chloride, copper chloride, iron chloride tetrahydrate, lactose, sodium hydroxide, thioacetamide (TAA), and acetone were purchased from Sigma Aldrich and used as received.

2.2. Synthesis of metal sulphide nanoparticles using lactose as capping agent

The nanoparticles were synthesised using a modified method described by Tan et al. [6]. Typically, 2.0 g of lactose were dissolved in 30 cm³ of distilled water at room temperature. About 5 cm³ of 0.744 M copper chloride was then added to the lactose solution and the pH of the reaction mixture was adjusted to 10 using sodium hydroxide solution followed by the addition of 5 cm³ of 1.33 M thioacetamide. The reaction mixture was then heated at 35 °C for an hour with vigorous stirring under nitrogen gas, after which a precipitate was formed. The mixture was then allowed to cool to room temperature and the precipitate was separated from the solution by centrifugation. The nanoparticles were washed several times with acetone and left overnight at room temperature to dry in a fume hood. Following the same procedure, copper sulphide nanoparticles were synthesized at different temperatures, i.e. 65 and 95 °C. The same method was used to prepare ZnS and FeS nanoparticles.

2.3.1. Solubility tests

About 0.0010 g of the nanoparticles synthesized at various temperatures was dissolved in 10 ml of water followed by sonication at room temperature for 15 minutes and centrifugation for 5 minutes at 2000 rpm. The dissolved particles were then decanted and the undissolved nanoparticles were allowed to dry overnight at room temperature. The mass was then weighed to establish the solubility of the particles by subtracting the mass of undissolved particles from the actual mass (0.0010 g).

3. Results and discussion

3.1. FT-IR spectroscopy analysis

The FT-IR spectra were recorded to study the interaction of the capping molecules with the surface of CuS, ZnS and FeS nanoparticles. In Fig. 1(a) lactose shows two bands between the regions of 3100-3400 cm⁻¹, emanating from the O-H group that is bonded to the ring carbon. One band around 3527 cm⁻¹ disappeared when lactose was bonded to the surface of the nanoparticles. The spectra of all nanoparticles showed a broad band at 3268 cm⁻¹ which can be attributed to adsorbed H₂O. The other difference observed is that, the spectra of all nanoparticles (Fig. 1(b-d)) showed a broad C-O stretch when compared to that of pure lactose. Upon interaction with the nanoparticles, the metal sulphide draws the electron density towards itself resulting in the weakening of the other bonds and thus their shifts and broadness in the spectra.

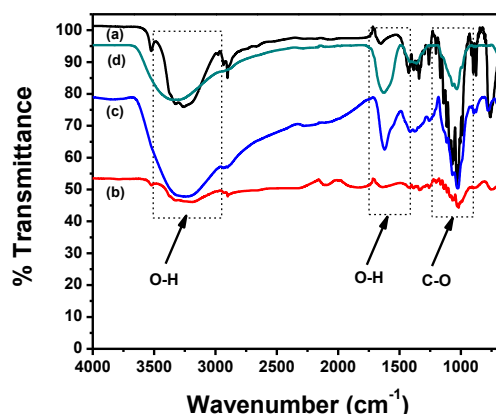


Fig. 1. Infrared spectra of (a) pristine lactose, (b) lactose-capped CuS nanoparticles, (c) lactose-capped ZnS nanoparticles and (d) lactose-capped FeS nanoparticles

3.2. Optical properties of lactose-capped ZnS and CuS nanoparticles

3.2.1. UV-Vis and PL spectroscopy

All metal sulphide nanoparticles were subjected to UV-Vis and PL spectroscopy analysis to study excitonic absorption and emission bands. The absorption spectra of the synthesized CuS nanoparticles at different temperatures are shown in Fig. 2(I). The optical properties of copper sulphide are rather fascinating; each stable phase displays its own characteristic properties for example, covellite CuS has a distinctive absorption peak in the near infra-red region at approximately 920 nm and this value decreases as the sulphur content increases from covellite to digenite ($\text{Cu}_{1.8}\text{S}$) to djurleite ($\text{Cu}_{1.96}\text{S}$) [7]. Chalcocite (Cu_2S) has been reported to have no apparent absorption. Compared to the bulk band-gap of copper sulphide (1022 nm), the spectra were blue-shifted and the absorption band-edges were approximately 541, 569, and 592 nm for particles synthesized at 35, 65 and 95 °C, respectively. The large blue-shift suggests that the particles were very small and therefore experienced stronger quantum confinement effects. The absorption red-shift as a function of temperature was attributed to Ostwald repining.

Fig. 2(II) shows the PL emission spectra of the lactose-capped CuS nanoparticles. The PL spectra were blue-shifted from the absorption band-edges and had emission maximum wavelengths at 390, 398 and 398 nm for particles synthesized at 35, 65 and 95 °C, respectively. This blue shift of emission spectra from the absorption edge is called photoluminescence up-conversion and it is a very rare phenomenon in optical studies of semiconductor nanomaterials. The cause of photoluminescence up-conversion was studied by Chen and co-workers [8] in ZnO nanoparticles and they reported that, processes known as two-photon-absorption and two step two-photon-absorption cause up-conversion due to surface defects or impurities with energy levels lying within 1.14-1.56 eV from one of the band edges without involving photon recycling[8]. All the emission peaks were broad indicating polydispersity.

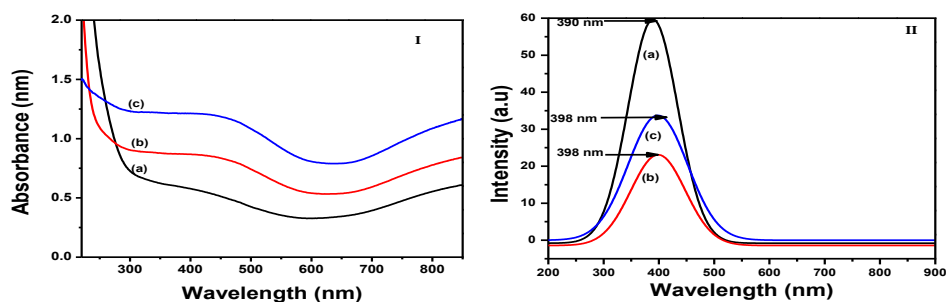


Fig. 2. Absorption (I) and emission (II) spectra of lactose capped-CuS nanoparticles synthesized at (a) 35°C, (b) 65°C, and (c) 95°C.

Fig. 3(I) shows absorption spectra of all lactose-capped ZnS nanoparticles. The absorption spectra of all samples showed a blue-shift in the absorption band edge compared to that of the bulk material (345 nm) [9], due to quantum confinement effects. For the lowest synthesis temperature (35 °C), the excitonic peak at 259 nm, which was at a shorter wavelength than 345 nm for bulk ZnS was observed and it was an indication of small sizes. This well-resolved exciton peak corresponds to the $1S_e-1S_h$ excitonic transitions in the ZnS nanoparticles [10]. There is also a sharp absorption edge at 335 nm, which is at a shorter wavelength than 345 nm of the bulk ZnS indicating small particle sizes. As the temperature was increased from 35 °C to 65 and 95 °C, the excitonic peaks started to disappear while the sharp absorption edges shifted to higher wavelength (339 & 342 nm). This shifting with increase in synthesis temperature suggests that the particles were becoming bigger in size and this could be attributed to Ostwald ripening. The sharp optical absorption edges and well defined excitonic feature indicate that the synthesized particles had relatively narrow size distributions.

The PL emission spectra of lactose-capped ZnS nanoparticles synthesized at different temperature are shown in Fig. 3(II). The emission spectra, which were red shifted from their absorption spectra, were all positioned at approximately 468 nm. The Full Width at Half Maximum (FWHM) was found to be 104, 107 and 108 nm for particles synthesized at 35, 65 and 95 °C, respectively. The FWHM showed narrower particle size distribution for all samples which is in agreement with UV-Vis spectroscopy analysis.

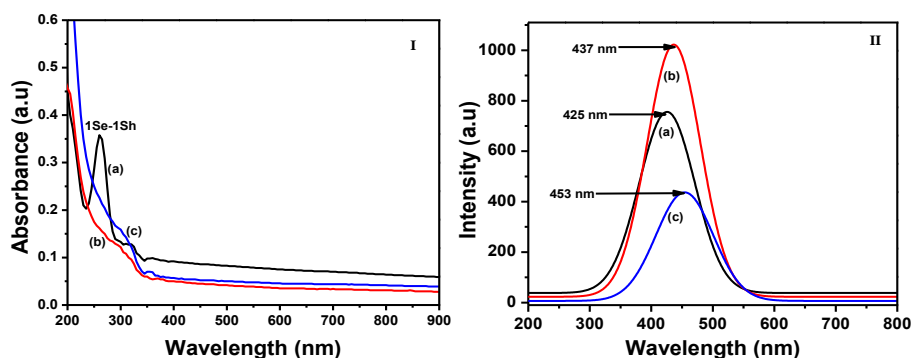


Fig. 3. Absorption (I) and emission (II) spectra of lactose capped-ZnS nanoparticles synthesized at (a) 35°C, (b) 65°C, and (c) 95°C

Fig 4(I) shows the UV-Vis absorption spectra of the lactose-capped FeS semiconductor nanoparticles synthesized at different temperatures. The absorption spectra of all samples showed a blue-shift in the absorption band edge compared to that of the bulk material, due to quantum confinement effects. All samples showed a shoulder like peak around 350 nm followed by tailing. The exact band gap edges could not be measured as there was a high degree of tailing for all samples. This high degree of tailing shows that the particles had a wide size distribution. Fig. 4(II) shows the room temperature PL excited at a wavelength of 275 nm for all samples. The PL spectra were red-shifted from their respective absorption spectra and the PL maxima were found to be 423, 408 and 421 nm for samples prepared at 35, 65 and 95 °C, respectively. All the emission peaks were broad signifying that the particles had broad size distribution. This was in agreement with the observed trends in the blue-shifts in the UV-Vis spectroscopic analysis.

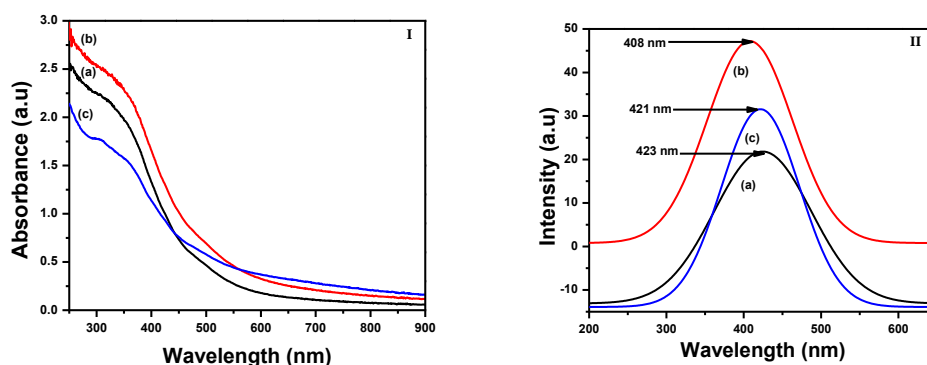


Fig. 4. Absorption (I) and emission (II) spectra of lactose capped-FeS nanoparticles synthesized at (a) 35°C, (b) 65°C, and (c) 95°C

3.3. XRD Analysis

The phase and crystallinity of the copper sulphide nanoparticles were determined by powder X-ray diffraction as shown in Fig. 5(I). The diffractograms were indexed to a hexagonal CuS (covellite) (JCPDS no: 06-0464) [11] and no traces of impurities were observed. As the temperature was increased, there was a sudden disappearance of some of the diffraction peaks at 65 and 95 °C which might be due to change in morphology.

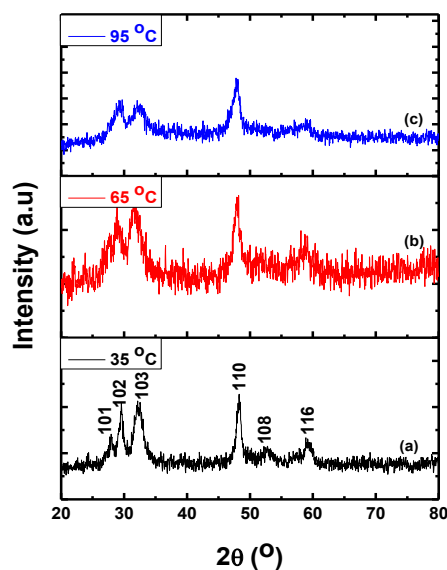


Fig. 5. XRD patterns of lactose capped-CuS nanoparticles prepared at temperatures of (a) 35 °C, (b) 65 °C, and (c) 95 °C

Fig. 6 shows the XRD patterns of lactose capped-ZnS nanoparticles. The patterns indicated that the synthesized nanoparticles were of cubic phase and the peak positions were in agreement with standard ZnS material [JCPDS 5-0566] [12]. There was no evidence of impurities observed from all samples. The broader peaks observed in the XRD pattern of the sample prepared at 35 °C suggest that the nanoparticles were of smaller size as compared to those prepared at 65 °C and 95°C. This could have been attributed to Ostwald ripening [13]. As the temperature was increased, the diffraction peaks became narrower indicating that the size of the nanoparticles was increasing. The crystalline size of ZnS semiconductor nanoparticles was calculated using Scherer's equation:

$$d = k\lambda / \beta \cos \theta \quad (1)$$

where “ d ” is the mean crystalline dimension, “ k ” is the crystallite shape constant (0.9), “ λ ” denotes the wavelength of the X-rays (Cu $K\alpha$: 1.5406Å), “ β ” is the full width at half maximum (FWHM) of the peak in radians, and “ θ ” is the diffraction angle, respectively. The average particle size was found to be 1.07, 2.75, and 2.95 nm for particles synthesized at 35, 65 and 95 °C, respectively. This increase in size with increase in reaction temperature is in agreement with UV-Vis spectroscopy analysis.

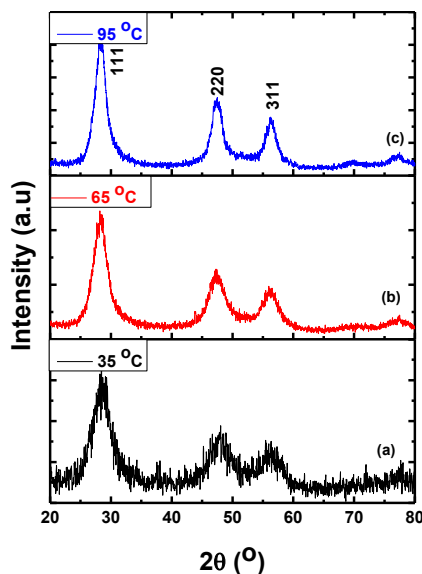


Fig. 6. XRD patterns of lactose capped-ZnS nanoparticles prepared at temperatures of (a) 35 °C, (b) 65 °C, and (c) 95 °C

The crystalline nature of the prepared lactose-capped FeS nanoparticles was confirmed by XRD. The XRD pattern for the sample prepared at 35 °C (Fig. 7(a)) showed that the sample was amorphous and as the temperature was increased to 65 and 95°C, the particles became crystalline. The amorphous nature of particles prepared at 35 °C might be due to the high decomposition temperature of lactose which is around 207 °C. The diffraction peaks at 2θ (23.0, 42.3, 56.2 and 62.1°) of high temperature samples correspond to a cubic greigite (Fe_3S_4) (ICDD No: 00-016-0713) [13] and lactose [14]. The increase in crystallinity was attributed to temperature which when increased might produce pure and high crystalline iron sulphide nanoparticles.

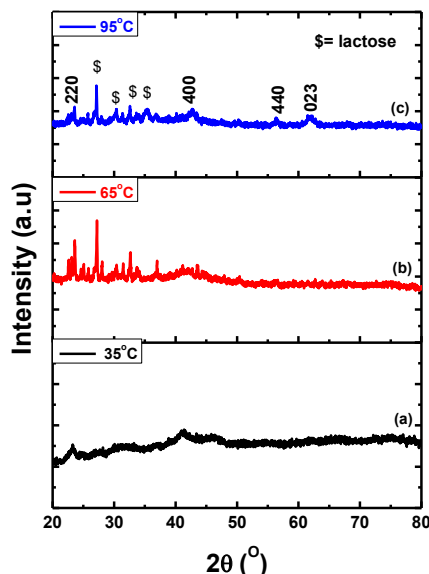


Fig. 7. XRD patterns of lactose capped-FeS nanoparticles prepared at temperatures of (a) 35 °C, (b) 65 °C, and (c) 95 °C

3.4. TEM Analysis

Fig 8 shows the TEM images of the lactose-capped CuS nanoparticles synthesized at 35, 65, and 95 °C. The sample synthesized at 35 °C had mixed morphology with fewer spherically shaped particles dominated by rod-shaped particles. As the temperature was increased, the particles became aggregated and formed nanoclusters. This change in morphology corroborates the XRD data.

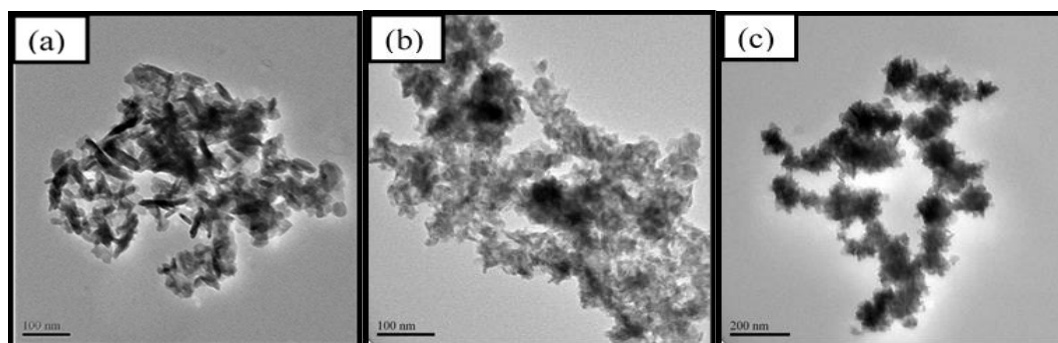


Fig. 8. TEM images of lactose-capped CuS nanoparticles synthesized at (a) 35 °C, (b) 65 °C, and (c) 95 °C.

The TEM images of lactose-capped ZnS nanoparticles are shown in Fig. 9. It can be seen from the TEM images that the particles are spherical in shape with some degree of aggregation in chain-like form. As the temperature was increased the morphology of the particles did not change. The particles were too small and hence it was difficult to estimate their sizes. The TEM images corroborate the data obtained from absorption and emission spectra.

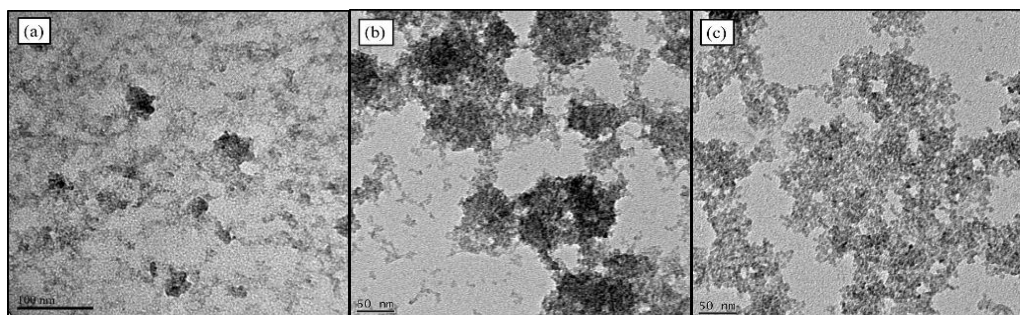


Fig. 9. TEM images lactose-capped ZnS nanoparticles prepared at (a) 35°C, (b) 65°C, and (c) 95°C

Fig. 10 shows the TEM images of lactose-capped FeS nanoparticles. The images show spherical shaped FeS nanoparticles with average particles size of 3.76, 3.99 and 5.22 nm for samples synthesized at 35, 65 and 95 °C, respectively. As the temperature was increased, the morphology of the particles did not change, however the particle size increased. These observed particle size increase with temperature can be attributed to the Ostwald ripening process.

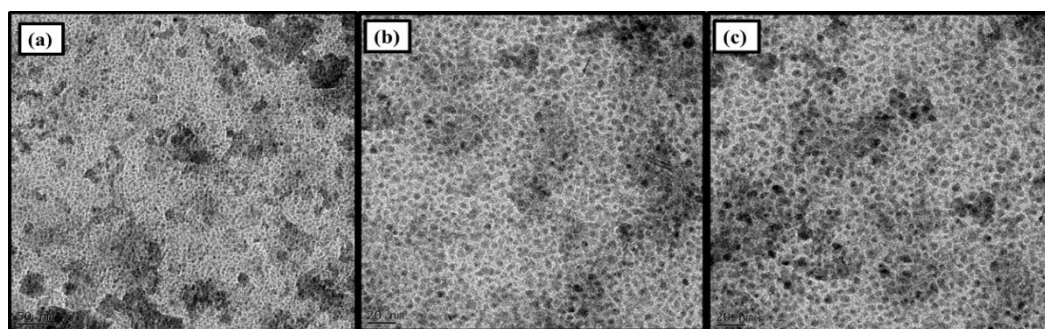


Fig. 10. TEM images lactose-capped FeS nanoparticles prepared 35°C (a), 65°C, (b) and 95°C (c).

3.5. Solubility tests

To further investigate the surface properties of the nanoparticles, a solubility test was performed. The solubility of CuS nanoparticles increased with an increase in synthetic temperature. This could be due to that at high temperature the capping agent bind strongly to the surface of the nanoparticles. As seen in optical and TEM results, the particles were aggregated and approached uniformity with increase in temperature. On the other hand, the solubility test for lactose capped-ZnS nanoparticles (Fig. 11(II)) showed no direct relationship between solubility and temperature increase. The nanoparticles synthesized at 35 °C were more soluble as compared to those synthesized at higher temperatures. As the temperature was increased, the solubility of the lactose-capped FeS nanoparticles also increased as shown in Fig. 11(III). This was attributed to the fact that at high temperature the capping agent binds more strongly to the surface of the nanoparticles.

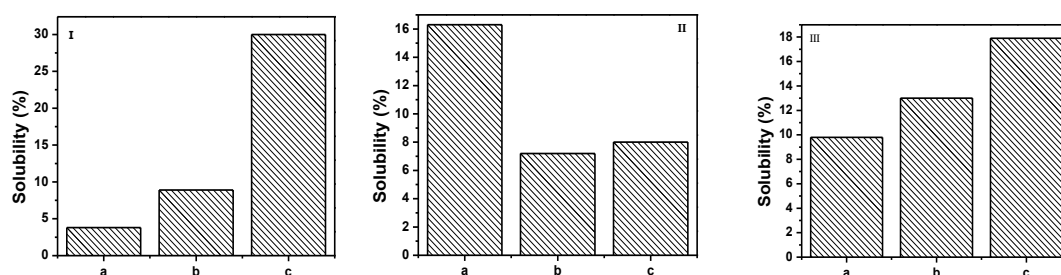


Fig. 11. Solubility graphs for CuS (I), ZnS (II), and FeS (III) nanoparticles prepared at (a) 35°C, (b) 65°C, and (c) 95°C

4. Conclusions

The relatively low temperatures used had effects on both the optical and morphological properties of nanoparticles. The increase in size of the nanoparticles with reaction temperature was associated with Ostwald ripening effects. For CuS and FeS nanoparticles, the highest synthetic temperature used in the study (95 °C) resulted in particles with narrow size distribution and high degree of water solubility compared to the ones synthesized at lower temperatures, and the surface coverage of the nanoparticles with lactose improved with increasing temperature as evidenced by the degree of water solubility of the particles. ZnS nanoparticles obtained at 35 °C were more soluble in water than those obtained at 95 °C.

Acknowledgements

The authors would like to acknowledge the National Research Foundation and Vaal University of Technology for financial support.

References

- [1] A.Z. Wang, R. Langer, O.C. Farokhzad, *Annu. Rev. Med.* **63**, 185 (2012).
- [2] J.R. Esparza, A. Martínez-mena, I. Gutiérrez-sancha, P. Rodríguez-fragoso, G. Gonzalez de la cruz, R. Mondragón, L. Rodríguez-fragoso, *J. Nanobiotechnology.* **13**, 1 (2015).
- [3] B. Kim, D.J. Hong, J. Bae, M. Lee, *J. Am. Chem. Soc.* **127**, 16333 (2005).
- [4] G. Barrientos, *Chem. Eur. J.* **9**, 1909 (2003).
- [5] K.K. Katti, V. Kattumuri, S. Bhaskaran, K.V. Katti, R. Kannan, *Int. J. Green Nanotechnol. Biomed.* **1** 53–59 (2009).
- [6] C. Tan, Y. Zhu, R. Lu, P. Xue, C. Bao, X. Liu, Z. Fei, Y. Zhao, *Mater. Chem. Phys.* **91**, 44 (2005).
- [7] S.K. Haram, A.R. Mahadeshwar, S.G. Dixit, *J. Phys. Chem.* **100**, 5868 (1996).
- [8] S. Chen, J.E. Stehr, N.K. Reddy, C.W. Tu, W. Chen, I. Buyanova, *Appl. Phys.* **4**, 919 (2012).
- [9] S. K. Maji, A. K. Dutta, D.N. Srivastava, P. Paul, A. Mondala, B. Adhikary, *Polyhedron.* **30**, 2493 (2011).
- [10] L. Wang, X.T. Tao, J.X. Yang, Y. Ren, Z. Liu, M.H. Jiang, *Opt. Mater.* **28**, 1080 (2006).
- [11] M. Saranya, C. Santhosh, R. Ramachandran, A.N. Grace, *Powder Technol.* **252**, 25 (2014).
- [12] A.A. Othman, M.A. Osman, M.H. Wahdan, A.G. Abed-elrahim, *Inter. J. Gen. Eng. Technol.* **3**, 9 (2014).
- [13] M. Akhtar, P.P. O'brien, School of chemistry. PhD thesis (2013).
- [14] K. Li, M.W. Woo, C. Selomulya, *J. Food Eng.* **169**, 196 (2016).